Journal of Computational and Applied Mathematics 231 (2009) 412–422

Contents lists available at ScienceDirect

Journal of Computational and Applied Mathematics

journal homepage: www.elsevier.com/locate/cam

Approximating tensor product Bézier surfaces with tangent plane continuity

Lizheng Lu

College of Statistics and Mathematics, Zhejiang Gongshang University, Hangzhou 310018, PR China

ARTICLE INFO

Article history:
Received 6 July 2008
Received in revised form 20 December 2008

Keywords:
Tensor product Bézier surfaces
Approximation
Degree reduction
L_2-norm
Tangent plane continuity

ABSTRACT

We present a simple method for degree reduction of tensor product Bézier surfaces with tangent plane continuity in L_2-norm. Continuity constraints at the four corners of surfaces are considered, so that the boundary curves preserve endpoints continuity of any order α. We obtain matrix representations for the control points of the degree reduced surfaces by the least-squares method. A simple optimization scheme that minimizes the perturbations of some related control points is proposed, and the surface patches after adjustment are C^∞ continuous in the interior and G^1 continuous at the common boundaries. We show that this scheme is applicable to surface patches defined on chessboard-like domains.

1. Introduction

Polynomial curves and surfaces in Bernstein–Bézier form are a widespread tool for the representations of curves and surfaces in CAGD (Computer Aided Geometric Design) [1]. They can be effectively evaluated by the de Casteljau algorithm and exhibit many elegant geometric properties, including the invariance under affine transformations, containment in the convex hull, and an intuitive geometric interpretation of the coefficients as control points.

Degree reduction of Bézier curves and surfaces is one of the most important approximation problems in CAGD and CAD/CAM. It consists of approximating a given curve or surface by another one of lower degree. The motivation for this research is the practical need to communicate product data between diverse systems that impose fundamentally incompatible constraints on their representation schemes. For example, some systems may restrict themselves to polynomial forms or limit the polynomial degrees that they can accommodate. Thus, there has been a lot of work on the degree reduction of Bézier curves [2–17] and of Bézier surfaces over rectangular [7,18,19], triangular [20–22] and simplex [23] domains.

Various norms have been used to measure the approximation error for degree reduction of polynomial curves. In L_∞-norm, the constrained degree reduction (with continuity constraints at the endpoints) was considered in [19] and [2] by using the Chebyshev and Jacobi polynomials, respectively. In L_2-norm, the Legendre–Bernstein basis transformation was used to give a simple solution for the unconstrained degree reduction [10], and the best constrained degree reduction was investigated in [3,14,17] by different approaches with the same results, which can be further improved by imposing geometric continuity instead of parametric continuity on the constraints [11]. In L_1-norm, the best one-sided approximation of polynomials was proposed and applied to degree reduction of interval Bézier curves [5].

While degree reduction of curves has been investigated extensively, very few studies have been carried out for surfaces. Due to the tensor product nature, it was outlined in [6,7] how one can solve in a very simple and straightforward manner the problem of degree reduction for tensor product Bézier surfaces once one has a suitable degree reduction method for Bézier curves. The main idea is to apply the curve algorithm, first to every row of the original control net and afterwards to

E-mail address: lulz99@yahoo.com.cn.

0377-0427/$ – see front matter © 2009 Elsevier B.V. All rights reserved.
doi:10.1016/j.cam.2009.03.007

every column of the resulting new control net. In [18], another different method, based on degree elevation of surfaces and Chebyshev polynomial approximation theory, was proposed. And the constrained Chebyshev economization was used for degree reduction of curves and surfaces in [19].

In this paper, we study the degree reduction problem of tensor product Bézier surfaces with tangent plane continuity. Similar to [18,21], the control net of every surface patch is divided into boundary control points and inner ones. Then the problem is solved in three steps. Firstly, the four boundary curves of each patch are degree reduced to a lower degree by the best C^α-constrained degree reduction method of curves in L_2-norm [3], so the boundary control points of approximating patches are obtained and any two adjacent patches will have a common boundary. Secondly, the inner control points of each approximating patch are obtained by minimizing the squared L_2-error with the boundary control points unchanged. They are expressed in matrix form without the use of degree elevation. Thirdly, a simple optimization scheme is proposed for two and four patches around a corner to satisfy the G^1 conditions, and it can be further extended to patches defined on chessboard-like domains. Some of the first two rings of control points from the boundaries are adjusted by optimizing their perturbations in the positions, which is decomposed into two kinds of minimization problems: three control points are arranged collinearly in a specific ratio, and nine control points are arranged collinearly in two specific ratios, cf. Fig. 3. The final patches of lower degree will be smoothly joined to form a globally G^1 surface.

2. Definitions and notations

Let $\mathbb{N}_0$ be the set of nonnegative integers. For $\mathbf{n} = (n_1, n_2) \in \mathbb{N}_0^2$, we sort all the indices $\mathbf{i} = (i_1, i_2) \in \mathbb{N}_0^2$ satisfying $i_1 \le n_1$ and $i_2 \le n_2$ in the following set

$$\Lambda^{\mathbf{n}} := \{(0,0), (1,0), \ldots, (n_1,0), (0,1), (1,1), \ldots, (n_1,1), \ldots, (0,n_2), (1,n_2), \ldots, (n_1,n_2)\},$$

which has $\mathrm{card}(\Lambda^{\mathbf{n}}) := (n_1+1)(n_2+1)$ elements. The addition and the binomial coefficient of two indices are expressed as

$$\mathbf{n} + \mathbf{i} := (n_1 + i_1, n_2 + i_2), \qquad \binom{\mathbf{n}}{\mathbf{i}} := \binom{n_1}{i_1}\binom{n_2}{i_2}.$$

Given the control points $\mathbf{p_i} \in \mathbb{R}^3$, the tensor product Bézier surface of degree $\mathbf{n}$ is defined by

$$\mathbf{P}(\mathbf{u}) = \sum_{\mathbf{i} \in \Lambda^{\mathbf{n}}} B_{\mathbf{i}}^{\mathbf{n}}(\mathbf{u})\mathbf{p_i}, \quad \mathbf{u} = (u, v) \in [0,1] \times [0,1], \tag{1}$$

where

$$B_{\mathbf{i}}^{\mathbf{n}}(\mathbf{u}) = B_{i_1}^{n_1}(u) B_{i_2}^{n_2}(v) = \binom{n_1}{i_1}\binom{n_2}{i_2}(1-u)^{n_1-i_1}u^{i_1}(1-v)^{n_2-i_2}v^{i_2}$$

are the generalized Bernstein basis functions of degree $\mathbf{n}$. These functions are nonnegative and form a partition of unity, i.e., $\sum_{\mathbf{i}\in\Lambda^{\mathbf{n}}} B_{\mathbf{i}}^{\mathbf{n}}(\mathbf{u}) = 1$. The summation contains $\mathrm{card}(\Lambda^{\mathbf{n}})$ linearly independent polynomials. See [1] for more details on the properties of the Bernstein form.

Let $\mathbf{B}^{\mathbf{n}} = \{B_{\mathbf{i}}^{\mathbf{n}}(\mathbf{u})\}_{\mathbf{i}\in\Lambda^{\mathbf{n}}}$ be the row vector of the Bernstein basis functions of degree $\mathbf{n}$, and $\mathbf{P}^{\mathbf{n}} = \{\mathbf{p_i}\}_{\mathbf{i}\in\Lambda^{\mathbf{n}}}^{\mathrm{T}}$ be the $\mathrm{card}(\Lambda^{\mathbf{n}}) \times 3$ matrix of the control points, where the order of every entry conforms to the order of its subscript $\mathbf{i}$ in $\Lambda^{\mathbf{n}}$. Then, the expression (1) can be rewritten in matrix form as

$$\mathbf{P}(\mathbf{u}) = \sum_{\mathbf{i}\in\Lambda^{\mathbf{n}}} B_{\mathbf{i}}^{\mathbf{n}}(\mathbf{u})\mathbf{p_i} = \mathbf{B}^{\mathbf{n}}\mathbf{P}^{\mathbf{n}}. \tag{2}$$

The product of two generalized Bernstein polynomials is also a generalized Bernstein polynomial and given by

$$B_{\mathbf{i}}^{\mathbf{n}}(\mathbf{u})B_{\mathbf{j}}^{\mathbf{m}}(\mathbf{u}) = \frac{\binom{\mathbf{n}}{\mathbf{i}}\binom{\mathbf{m}}{\mathbf{j}}}{\binom{\mathbf{n}+\mathbf{m}}{\mathbf{i}+\mathbf{j}}} B_{\mathbf{i}+\mathbf{j}}^{\mathbf{n}+\mathbf{m}}(\mathbf{u}), \quad \mathbf{i} \in \Lambda^{\mathbf{n}}, \ \mathbf{j} \in \Lambda^{\mathbf{m}}. \tag{3}$$

Lemma 1. *For all $\mathbf{i} \in \Lambda^{\mathbf{n}}$, the Bernstein basis functions of degree $\mathbf{n}$ satisfy*

$$\int_0^1\int_0^1 B_{\mathbf{i}}^{\mathbf{n}}(\mathbf{u})\mathrm{d}u\mathrm{d}v = \frac{1}{\mathrm{card}(\Lambda^{\mathbf{n}})}. \tag{4}$$

Lemma 2. *Let $\mathbf{G}_{\mathbf{n},\mathbf{m}} = \left(g_{\mathbf{i},\mathbf{j}}\right)$ be a $\mathrm{card}(\Lambda^{\mathbf{n}}) \times \mathrm{card}(\Lambda^{\mathbf{m}})$ matrix with the elements given by*

$$g_{\mathbf{i},\mathbf{j}} = \int_0^1\int_0^1 B_{\mathbf{i}}^{\mathbf{n}}(\mathbf{u})B_{\mathbf{j}}^{\mathbf{m}}(\mathbf{u})\mathrm{d}u\mathrm{d}v = \frac{1}{\mathrm{card}(\Lambda^{\mathbf{n}+\mathbf{m}})} \times \frac{\binom{\mathbf{n}}{\mathbf{i}}\binom{\mathbf{m}}{\mathbf{j}}}{\binom{\mathbf{n}+\mathbf{m}}{\mathbf{i}+\mathbf{j}}}, \quad \mathbf{i} \in \Lambda^{\mathbf{n}}, \ \mathbf{j} \in \Lambda^{\mathbf{m}}. \tag{5}$$

Then, $\mathbf{G}_{\mathbf{m},\mathbf{m}}$ is a real symmetric positive definite matrix.

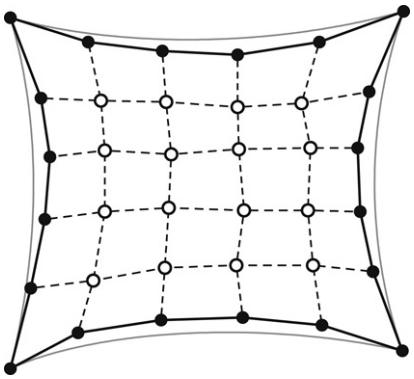

Fig. 1. Two steps for the constrained degree reduction.

Proof. Obviously, we can derive (5) from (3) and (4). For any nonzero column vector $\boldsymbol{\xi}$ with card$(\Lambda^{\mathbf{m}})$ elements, we have

$$\int_0^1 \int_0^1 \left(\sum_{\mathbf{i} \in \Lambda^{\mathbf{m}}} B_{\mathbf{i}}^{\mathbf{m}}(\mathbf{u}) \boldsymbol{\xi}_{\mathbf{i}} \right)^2 \mathrm{d}u\mathrm{d}v = \boldsymbol{\xi}^{\mathrm{T}} \mathbf{G}_{\mathbf{m},\mathbf{m}} \boldsymbol{\xi} > 0. \quad \square$$

3. Degree reduction with common boundaries

Given the control points $\mathbf{P}^{\mathbf{n}} = \{\mathbf{p}_{\mathbf{i}}\}^{\mathrm{T}}_{\mathbf{i} \in \Lambda^{\mathbf{n}}}$, a tensor product Bézier surface of degree $\mathbf{n}$ can be expressed as

$$\mathbf{P}(\mathbf{u}) = \mathbf{B}^{\mathbf{n}} \mathbf{P}^{\mathbf{n}}.$$

The problem of degree reduction is to find the control points $\mathbf{Q}^{\mathbf{m}} = \{\mathbf{q}_{\mathbf{j}}\}^{\mathrm{T}}_{\mathbf{j} \in \Lambda^{\mathbf{m}}}$, which define the approximating tensor product Bézier surface

$$\mathbf{Q}(\mathbf{u}) = \mathbf{B}^{\mathbf{m}} \mathbf{Q}^{\mathbf{m}}$$

of lower degree $\mathbf{m}$ ($m_1 < n_1$ and $m_2 < n_2$), such that the squared L_2-error ε is minimized. Here ε, based on the L_2-norm between two surfaces, is defined by

$$\varepsilon = \int_0^1 \int_0^1 \|\mathbf{P}(\mathbf{u}) - \mathbf{Q}(\mathbf{u})\|^2 \, \mathrm{d}u\mathrm{d}v. \tag{6}$$

We consider the constraints that the corresponding boundary curves have endpoints continuity of any order α ($\alpha \geq 0$). The process of degree reduction consists of two steps:

(1) Boundary curves approximation (Section 3.1): for the two boundary curves of degree n_1 (respectively n_2) of the surface $\mathbf{P}(\mathbf{u})$, find two approximating curves of degree m_1 (respectively m_2), having the same derivatives up to order α at the endpoints.
(2) Constrained surface approximation (Section 3.2): with the boundary control points calculated above, obtain the inner control points by the constrained least-squares method.

Fig. 1 demonstrates the two steps of degree reduction. After getting the black dots ($\bullet$) from Step 1, we obtain the hollow circles ($\circ$) from Step 2. Finally, we obtain the whole control net of the approximating surface $\mathbf{Q}(\mathbf{u})$.

3.1. Boundary curves approximation

There are four boundary curves to the given surface $\mathbf{P}(\mathbf{u})$:

$$\mathbf{P}^{v=0}(u) = \sum_{i=0}^{n_1} B_i^{n_1}(u) \mathbf{p}_{(i,0)}, \qquad \mathbf{P}^{v=1}(u) = \sum_{i=0}^{n_1} B_i^{n_1}(u) \mathbf{p}_{(i,n_2)}, \quad u \in [0,1],$$

$$\mathbf{P}^{u=0}(v) = \sum_{j=0}^{n_2} B_j^{n_2}(v) \mathbf{p}_{(0,j)}, \qquad \mathbf{P}^{u=1}(v) = \sum_{j=0}^{n_2} B_j^{n_2}(v) \mathbf{p}_{(n_1,j)}, \quad v \in [0,1].$$

The problem is now to construct the four approximating curves with endpoints continuity of order α.

The best C^{α}-constrained degree reduction of polynomial curves in L_2-norm is a classical problem in CAGD. Many methods have been developed to tackle it, see e.g. [3,7,11,14,17]. And the method in [11] produces better approximation than other

methods, since the constraints of geometric continuity will give additional parameters to optimize the approximation. However, it is somewhat complicated because the solution is achieved by numerical iterative methods. Therefore, in this paper, we use the method in [3], which proved that the best weighted Euclidean approximation of Bézier coefficients provides the best C^α-constrained degree reduction of Bézier curves in L_2-norm.

3.2. Constrained surface approximation

In order to distinguish the calculated control points from the unknown ones, we divide the set $\Lambda^{\mathbf{m}}$ into two subsets, i.e.,

$$\Lambda^{\mathbf{m}} = \Lambda_c^{\mathbf{m}} \cup \Lambda_f^{\mathbf{m}},$$

where

$$\Lambda_c^{\mathbf{m}} = \{(i_1, i_2) \in \Lambda^{\mathbf{m}} : i_1 = 0 \text{ or } i_2 = 0 \text{ or } i_1 = m_1 \text{ or } i_2 = m_2\}$$

is the union of all the corresponding indices of the boundary control points, and $\Lambda_f^{\mathbf{m}} = \Lambda^{\mathbf{m}} \setminus \Lambda_c^{\mathbf{m}}$ is its complement. Let

$$\mathbf{Q}^{\mathbf{m}} = \mathbf{Q}_c^{\mathbf{m}} \cup \mathbf{Q}_f^{\mathbf{m}} = \{\mathbf{q_i} \in \mathbf{Q}^{\mathbf{m}} : \mathbf{i} \in \Lambda_c^{\mathbf{m}}\} \cup \{\mathbf{q_i} \in \mathbf{Q}^{\mathbf{m}} : \mathbf{i} \in \Lambda_f^{\mathbf{m}}\},$$

where $\mathbf{Q}_c^{\mathbf{m}}$ and $\mathbf{Q}_f^{\mathbf{m}}$ denote the boundary and inner control points, respectively.

We now have to determine $\mathbf{Q}_f^{\mathbf{m}}$. We use the least-squares method to solve it, see e.g. [24]. Recall that our goal is to minimize the squared L_2-error

$$\begin{aligned}\varepsilon &= \int_0^1 \int_0^1 \|\mathbf{P}(\mathbf{u}) - \mathbf{Q}(\mathbf{u})\|^2 \, du dv \\ &= \int_0^1 \int_0^1 \left\| \mathbf{B}^{\mathbf{n}}\mathbf{P}^{\mathbf{n}} - \mathbf{B}_c^{\mathbf{m}}\mathbf{Q}_c^{\mathbf{m}} - \mathbf{B}_f^{\mathbf{m}}\mathbf{Q}_f^{\mathbf{m}} \right\|^2 du dv. \end{aligned} \tag{7}$$

Taking the partial derivatives of (7) with respect to $\mathbf{q_i}$ ($\mathbf{i} \in \mathbf{Q}_f^{\mathbf{m}}$) and setting the derivatives equal to zero lead to the normal equations

$$\int_0^1 \int_0^1 B_{\mathbf{i}}^{\mathbf{m}}(\mathbf{u}) \left(\mathbf{B}^{\mathbf{n}}\mathbf{P}^{\mathbf{n}} - \mathbf{B}_c^{\mathbf{m}}\mathbf{Q}_c^{\mathbf{m}} - \mathbf{B}_f^{\mathbf{m}}\mathbf{Q}_f^{\mathbf{m}} \right) du dv = \mathbf{0}, \quad \mathbf{i} \in \mathbf{Q}_f^{\mathbf{m}}. \tag{8}$$

Finally, we rewrite (8) into matrix form

$$\mathbf{G}_{ff}\mathbf{Q}_f^{\mathbf{m}} = \mathbf{G}_f\mathbf{P}^{\mathbf{n}} - \mathbf{G}_{fc}\mathbf{Q}_c^{\mathbf{m}}, \tag{9}$$

where

$$\mathbf{G}_{ff} := \mathbf{G}_{\mathbf{m},\mathbf{m}}\left(\Lambda_f^{\mathbf{m}}; \Lambda_f^{\mathbf{m}}\right), \qquad \mathbf{G}_f := \mathbf{G}_{\mathbf{m},\mathbf{n}}\left(\Lambda_f^{\mathbf{m}}; \Lambda^{\mathbf{n}}\right), \qquad \mathbf{G}_{fc} := \mathbf{G}_{\mathbf{m},\mathbf{m}}\left(\Lambda_f^{\mathbf{m}}; \Lambda_c^{\mathbf{m}}\right).$$

The notation $\mathbf{A}(\ldots;\ldots)$ denotes the submatrix of the matrix $\mathbf{A}$ obtained by extracting the specific rows and columns.

Since the matrix $\mathbf{G}_{\mathbf{m},\mathbf{m}}$ is a real symmetric positive definite matrix (see Lemma 2), $\mathbf{G}_{ff}$ is invertible. Therefore, (7) is minimized by choosing

$$\mathbf{Q}_f^{\mathbf{m}} = \left(\mathbf{G}_{ff}\right)^{-1}\left(\mathbf{G}_f\mathbf{P}^{\mathbf{n}} - \mathbf{G}_{fc}\mathbf{Q}_c^{\mathbf{m}}\right). \tag{10}$$

Theorem 1. *The squared L_2-error for the degree reduction is given by*

$$\varepsilon = (\mathbf{P}^{\mathbf{n}})^{\mathrm{T}}\mathbf{G}_{\mathbf{n},\mathbf{n}}\mathbf{P}^{\mathbf{n}} - 2(\mathbf{P}^{\mathbf{n}})^{\mathrm{T}}\mathbf{G}_{\mathbf{n},\mathbf{m}}\mathbf{Q}^{\mathbf{m}} + (\mathbf{Q}^{\mathbf{m}})^{\mathrm{T}}\mathbf{G}_{\mathbf{m},\mathbf{m}}\mathbf{Q}^{\mathbf{m}}. \tag{11}$$

Remark 1. If a user-prescribed tolerance should be fulfilled, one has to combine degree reduction with surface subdivision. When $\alpha \geq 0$, the piecewise tensor product Bézier surfaces are C^0 continuous on the boundary curves and C^∞ continuous in the interior; when $\alpha = 1$, the tangent planes at the corners are also continuous; when $\alpha > 1$, the order of continuity on the boundary curves does not increase any more. Therefore, if one starts with several smoothly joined surface patches and applies degree reduction to each one, piecewise continuous approximations are obtained without undesirable gaps.

4. Tangent plane continuity at common boundaries

After the constrained degree reduction by Section 3, any two adjacent surface patches will share a common boundary curve. However, in practical applications, only positional continuity is not satisfactory, see Fig. 5 for an illustration. So,

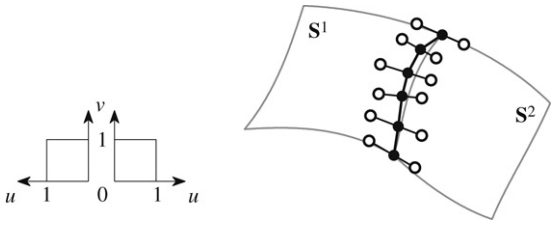

Fig. 2. Parameterization of two surface patches with a common boundary.

we require the approximating surfaces to have continuously varying tangent planes along common boundaries, i.e., G^1 continuous. This means that the surfaces are C^∞ everywhere except at the inner patch boundaries.

Geometric continuity between two tensor product Bézier surfaces has been widely investigated (see e.g. [1,25–27], where necessary and sufficient conditions are derived and discussed). They mostly give a system of conditions of the form: Two adjacent patches are smoothly joined with G^n continuity if and only if there exist parameters such that a certain set of equations are satisfied. In particular, DeRose [25] provided a set of conditions related only to the placement of control points to judge whether or not two patches are G^1 continuous. However, our goal is to perturb some related control points such that adjacent patches have continuously varying tangent planes along common boundaries. Therefore, their conditions are not in a form that is convenient for the current study. In this section, we will present a simple method to optimize the perturbations of control points to satisfy the requirement of tangent plane continuity.

4.1. G^1 conditions between two surface patches

Let $\mathbf{S}^1$ and $\mathbf{S}^2$ be two adjacent tensor product Bézier patches parameterized as in Fig. 2. They join at the common boundary with tangent plane continuity if and only if there exist two scalar functions such that

$$\frac{\partial \mathbf{S}^2}{\partial u}(0, v) + \lambda(v)\frac{\partial \mathbf{S}^1}{\partial u}(0, v) + \nu(v)\frac{\partial \mathbf{S}^1}{\partial v}(0, v) = 0, \tag{12}$$

where $\lambda(v) > 0$ is assumed to avoid ridges.

We now consider a simple case of (12) by taking the scalar functions as follows:

$$\lambda(v) = \lambda > 0, \qquad \nu(v) = 0.$$

Then, it becomes

$$\frac{\partial \mathbf{S}^2}{\partial u}(0, v) = -\lambda\frac{\partial \mathbf{S}^1}{\partial u}(0, v). \tag{13}$$

It is obvious that when $\lambda = 1$, the concept of G^1 continuity degenerates to C^1.

Without loss of generality, we assume that the degree of the common boundary curve is n, and represent it in Bernstein form

$$\mathbf{S}^1(0, v) = \mathbf{S}^2(0, v) = \sum_{i=0}^{n} B_i^n(v)\mathbf{b}_i, \quad v \in [0, 1].$$

Denote the first inner column control points of $\mathbf{S}^1$ from the common boundary by $\mathbf{a}_0, \ldots, \mathbf{a}_n$, and those of $\mathbf{S}^2$ by $\mathbf{c}_0, \ldots, \mathbf{c}_n$. We then express (13) as

$$\sum_{i=0}^{n} B_i^n(v)(\mathbf{c}_i - \mathbf{b}_i) = -\lambda\sum_{i=0}^{n} B_i^n(v)(\mathbf{a}_i - \mathbf{b}_i),$$

which is equivalent to (due to the linear independence of the Bernstein basis)

$$\mathbf{c}_i - \mathbf{b}_i = \lambda(\mathbf{b}_i - \mathbf{a}_i), \quad i = 0, 1, \ldots, n. \tag{14}$$

The constant λ in (13) and (14) controls the ratio of the three points $\mathbf{a}_i$, $\mathbf{b}_i$ and $\mathbf{c}_i$. And (14) implies that if $\mathbf{a}_i$, $\mathbf{b}_i$ and $\mathbf{c}_i$ are collinear and in the same ratio for all i (cf. Fig. 2), then $\mathbf{S}^1$ and $\mathbf{S}^2$ are G^1 continuous and thus have continuous tangent planes along the common boundary.

Remark 2. If $\mathbf{S}^1$ and $\mathbf{S}^2$ satisfy the conditions (14), then we can find a linear map,

$$\phi\colon [0, 1] \times [0, 1] \mapsto [0, \lambda] \times [0, 1], \quad \phi(u, v) = (\lambda u, v),$$

such that $\mathbf{S}^1(u, v)$ and $\mathbf{S}^2(\phi(u, v))$ are joined with C^1 continuity.

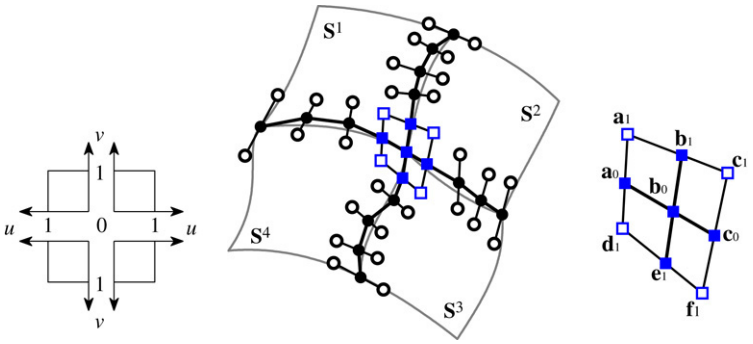

Fig. 3. Parameterization of four surface patches and the control points related to the twists at the corner $\mathbf{b}_0$.

For two adjacent patches with a common boundary, the conditions (14) may be not satisfied. Our main idea is to perturb the control points $\mathbf{a}_i$ and $\mathbf{c}_i$ if needed to meet all the conditions. At first, we determine λ from the optimization problem:

$$\min_{\lambda} \sum_{i=0}^{n} w_i \left(\frac{\|\mathbf{c}_i - \mathbf{b}_i\|}{\|\mathbf{b}_i - \mathbf{a}_i\|} - \lambda \right)^2, \tag{15}$$

where

$$w_i = \begin{cases} \left(\dfrac{n-i}{n} \right)^2, & i \le \left\lfloor \dfrac{n}{2} \right\rfloor, \\ \left(\dfrac{i}{n} \right)^2, & i > \left\lfloor \dfrac{n}{2} \right\rfloor. \end{cases}$$

The weights w_i are used to preserve important features near the two endpoints. Obviously, the solution of (15) is

$$\lambda = \frac{1}{\sum_{i=0}^{n} w_i} \sum_{i=0}^{n} w_i \frac{\|\mathbf{c}_i - \mathbf{b}_i\|}{\|\mathbf{b}_i - \mathbf{a}_i\|}. \tag{16}$$

Next, we have to fix the new positions of $\mathbf{a}_i$ and $\mathbf{c}_i$ for all i, denoted as $\bar{\mathbf{a}}_i$ and $\bar{\mathbf{c}}_i$. By the ratio, we have

$$\bar{\mathbf{c}}_i = -\lambda \bar{\mathbf{a}}_i + (1+\lambda)\mathbf{b}_i. \tag{17}$$

Then, $\bar{\mathbf{a}}_i$ is obtained in the sense of minimizing the perturbations

$$\|\mathbf{a}_i - \bar{\mathbf{a}}_i\|^2 + \|\mathbf{c}_i - \bar{\mathbf{c}}_i\|^2 = \|\mathbf{a}_i - \bar{\mathbf{a}}_i\|^2 + \|\mathbf{c}_i - (1+\lambda)\mathbf{b}_i + \lambda \bar{\mathbf{a}}_i\|^2.$$

And the solution is

$$\bar{\mathbf{a}}_i = \frac{\mathbf{a}_i + \lambda(1+\lambda)\mathbf{b}_i - \lambda \mathbf{c}_i}{1+\lambda^2}, \qquad \bar{\mathbf{c}}_i = \frac{-\lambda \mathbf{a}_i + (1+\lambda)\mathbf{b}_i + \lambda^2 \mathbf{c}_i}{1+\lambda^2}. \tag{18}$$

At the patch corner ($(u, v) = (0, 0)$ or $(0, 1)$), the G^1 continuity is directly related to the twists. Therefore, the following necessary conditions of G^1-continuity, called compatibility conditions (refer to [1, Section 22.6]), must hold:

$$\frac{\partial^2 \mathbf{S}^2}{\partial u \partial v}(0, v) = -\lambda \frac{\partial^2 \mathbf{S}^1}{\partial u \partial v}(0, v), \quad v = 0, 1. \tag{19}$$

Take the corner at $(u, v) = (0, 0)$ for example. To satisfy (19), we have to verify that

$$(\bar{\mathbf{c}}_1 - \bar{\mathbf{c}}_0) - (\mathbf{b}_1 - \mathbf{b}_0) = -\lambda\big((\bar{\mathbf{a}}_1 - \bar{\mathbf{a}}_0) - (\mathbf{b}_1 - \mathbf{b}_0)\big),$$

which is a result of (17).

4.2. G^1 conditions between four surface patches

We consider four adjacent tensor product Bézier patches around the corner $\mathbf{b}_0$, see Fig. 3. Let us start with discussing the G^1 join along the v-direction at $u = 0$. $\mathbf{S}^1$ and $\mathbf{S}^2$ are G^1 continuous if the conditions (14) are satisfied. Denote the control points of $\mathbf{S}^4(0, v)$ by $\mathbf{e}_0, \ldots, \mathbf{e}_n$, and denote the first inner column control points of $\mathbf{S}^4$ from the common boundary by $\mathbf{d}_0, \ldots, \mathbf{d}_n$ and those of $\mathbf{S}^3$ by $\mathbf{f}_0, \ldots, \mathbf{f}_n$. Then, the G^1 conditions at the boundaries $u = 0$ become

$$\mathbf{c}_i - \mathbf{b}_i = \lambda(\mathbf{b}_i - \mathbf{a}_i), \qquad \mathbf{f}_i - \mathbf{e}_i = \lambda(\mathbf{e}_i - \mathbf{d}_i), \quad i = 0, 1, \ldots, n. \tag{20}$$

Usually, the values of λ, computed by (16), may be different for the boundary of $\mathbf{S}^1$ and $\mathbf{S}^2$ and that of $\mathbf{S}^4$ and $\mathbf{S}^3$. We suggest to take their average. However, it is possible that the difference (in the form of standard deviation, for example) may be very big in some worst cases, especially when the boundaries are composed by more than two segments. If this happens, we divide the boundaries into some continuous groups collected according to the values of λ, and every two groups will be separated by one or several segments. This scheme can better preserve the features of patches. But, since the adjustment is applied after degree reduction, the difference will be small when the original surface patches are smoothly joined.

Similar to (20), the G^1 conditions can be derived for the u-direction. Denote by μ the ratio at the boundaries $v = 0$. We thus have

$$\mathbf{d}_1 - \mathbf{a}_0 = \mu(\mathbf{a}_0 - \mathbf{a}_1), \qquad \mathbf{e}_1 - \mathbf{b}_0 = \mu(\mathbf{b}_0 - \mathbf{b}_1), \qquad \mathbf{f}_1 - \mathbf{c}_0 = \mu(\mathbf{c}_0 - \mathbf{c}_1). \tag{21}$$

Now, we begin to adjust the positions of some control points to satisfy (20) and (21). First of all, since $\mathbf{a}_0$, $\mathbf{b}_0$, $\mathbf{c}_0$ and $\mathbf{b}_1$, $\mathbf{b}_0$, $\mathbf{e}_1$ are collinear with the ratios λ and μ respectively, these points (marked by ■ in Fig. 3) must be coplanar. Otherwise, we adjust the positions for $\mathbf{a}_0$, $\mathbf{c}_0$, $\mathbf{b}_1$ and $\mathbf{e}_1$ by (18), and denote them by $\bar{\mathbf{a}}_0$, $\bar{\mathbf{c}}_0$, $\bar{\mathbf{b}}_1$ and $\bar{\mathbf{e}}_1$.

Secondly, we have to determine the new positions for all the points marked by □ in Fig. 3, denoted by $\bar{\mathbf{a}}_1$, $\bar{\mathbf{c}}_1$, $\bar{\mathbf{d}}_1$ and $\bar{\mathbf{f}}_1$. From the conditions (20) and (21), we have the following equations:

$$\begin{aligned}
&\bar{\mathbf{c}}_1 = -\lambda\bar{\mathbf{a}}_1 + (1+\lambda)\bar{\mathbf{b}}_1,\\
&\bar{\mathbf{d}}_1 = -\mu\bar{\mathbf{a}}_1 + (1+\mu)\bar{\mathbf{a}}_0,\\
&\bar{\mathbf{f}}_1 = \lambda\mu\bar{\mathbf{a}}_1 - \lambda(1+\mu)\bar{\mathbf{a}}_0 + (1+\lambda)\bar{\mathbf{e}}_1 = \lambda\mu\bar{\mathbf{a}}_1 - \mu(1+\lambda)\bar{\mathbf{b}}_1 + (1+\mu)\bar{\mathbf{c}}_0.
\end{aligned} \tag{22}$$

We optimize $\bar{\mathbf{a}}_1$ by minimizing the perturbations

$$\begin{aligned}
&\|\mathbf{a}_1 - \bar{\mathbf{a}}_1\|^2 + \|\mathbf{c}_1 - \bar{\mathbf{c}}_1\|^2 + \|\mathbf{d}_1 - \bar{\mathbf{d}}_1\|^2 + \|\mathbf{f}_1 - \bar{\mathbf{f}}_1\|^2 = \|\mathbf{a}_1 - \bar{\mathbf{a}}_1\|^2 + \|\mathbf{c}_1 - (1+\lambda)\bar{\mathbf{b}}_1 + \lambda\bar{\mathbf{a}}_1\|^2\\
&\quad + \|\mathbf{d}_1 - (1+\mu)\bar{\mathbf{a}}_0 + \mu\bar{\mathbf{a}}_1\|^2 + \|\mathbf{f}_1 + \lambda(1+\mu)\bar{\mathbf{a}}_0 - (1+\lambda)\bar{\mathbf{e}}_1 - \lambda\mu\bar{\mathbf{a}}_1\|^2,
\end{aligned}$$

with the solution given by

$$\bar{\mathbf{a}}_1 = \frac{\mathbf{a}_1 - \lambda\mathbf{c}_1 - \mu\mathbf{d}_1 + \lambda\mu\mathbf{f}_1 + \lambda(1+\lambda)\bar{\mathbf{b}}_1 + \mu(1+\lambda^2)(1+\mu)\bar{\mathbf{a}}_0 - \lambda\mu(1+\lambda)\bar{\mathbf{e}}_1}{(1+\lambda^2)(1+\mu^2)}. \tag{23}$$

And the new positions of $\bar{\mathbf{c}}_1$, $\bar{\mathbf{d}}_1$ and $\bar{\mathbf{f}}_1$ are obtained by substituting (23) into (22).

Finally, we determine all the other related points (marked by • and ∘ in Fig. 3) by using (18) (replacing λ with μ for the u-direction).

It is easy to verify that compatibility conditions such as (19) hold at $\mathbf{b}_0$ and the other four corners in Fig. 3, due to (20) and (21).

Remark 3. Assume that the four surface patches in Fig. 3 are defined on the domain $[-1, 0] \cup [0, \lambda] \times [-\mu, 0] \cup [0, 1]$. Then they form C^1 continuous Bézier spline surfaces, if the conditions (20) of the v-direction and the counterparts of the u-direction including (21) are satisfied. In fact, a similar result also exists for surface patches defined on chessboard-like domains: They will be joined to form a globally G^1 surface (C^1, after linear maps of the domain) when all the inner u- and v-directions conform to the G^1 conditions like (20).

5. Examples

Example 1. A tensor product Bézier surface of degree (6, 6) is shown in Fig. 4, with its control points given by $\mathbf{P}^{(6,6)} =$ {(0, 0, 0.8), (0.2, 0.8, 1.8), (0.5, 2.1, 2.3), (0.3, 3.2, 1.6), (0, 3.8, 0.2), (0.2, 4.8, −1.2), (0.5, 5.5, −1.7), (1, −0.7, 1.6), (1.2, 0.6, 2.2), (1, 1.6, 2.4), (0.7, 2.5, 1.6), (1, 3.4, 0), (1.3, 4.3, −0.45), (1.4, 4.4, −0.8), (2.3, 0.55, 2.1), (2.1, 1.4, 3.2), (1.6, 2.4, 3.6), (1.9, 3.4, 2.4), (2.2, 4.7, 1.3), (1.8, 5.5, 0.2), (1.5, 4.7, −1.8), (3.1, 0.2, −2.8), (3.2, 0.8, 1.2), (3.1, 2.2, 2.1), (2.8, 3.2, 0.2), (2.6, 4.1, −0.4), (3.1, 4.8, −2.8), (2.8, 5, −3.2), (3.6, −0.6, 0.1), (3.9, 0.3, 0.9), (4, 1.2, 1.2), (3.9, 2.2, 1.2), (3.6, 3.3, 0.1), (3.6, 4.3, −1.1), (3.9, 4.6, −1.1), (5.1, 0.1, −0.6), (5.5, 1.1, 0.1), (5.6, 2.3, 1.1), (5.1, 3.1, 2.2), (4.9, 4.1, 1.1), (4.6, 5.1, −0.8), (4.8, 5.2, −1.8), (6.4, 0.8, −0.1), (6.4, 1.6, 1.2), (6.7, 2.7, 2.5), (6.4, 3.6, 3.2), (6.3, 4.6, 1.7), (5.9, 4.9, −0.6), (5.7, 6, −1.2)}.

We subdivide the surface at the domain point (0.5, 0) using the de Casteljau algorithm [1], and then reduce the degree to (4, 4) by the method in Section 3 with $\alpha = 1$. The result is shown in Fig. 5(a). Clearly, the approximation effect is unsatisfactory, since the degree reduction can only achieve the same positions at the common boundary. Then, we further adjust a column of control points of either patch by the scheme in Section 4.1, with the improved result in Fig. 5(b). And the maximum L_2-errors (i.e., $\sqrt{\varepsilon}$ of (11)) of the two pairs of patches are 0.071 and 0.161, respectively. Therefore, we obtain a satisfactory approximation since the two patches have continuously varying tangent planes, at the cost of the increase of approximation error. A better approximation is provided in Fig. 5(c), where the four patches are obtained by subdividing the original surface at the domain point (0.5, 0.5) and using the scheme in Section 4.2 after degree reduction. The maximum L_2-error of the four pairs of patches is 0.011.

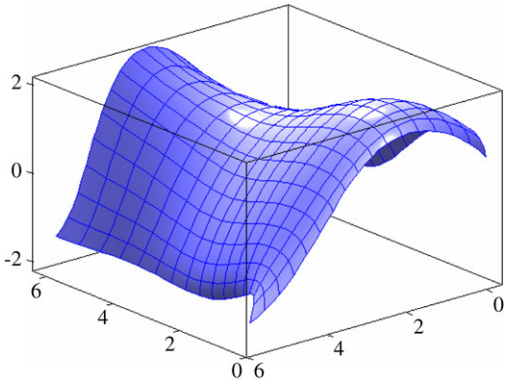

Fig. 4. The surface patch given in Example 1.

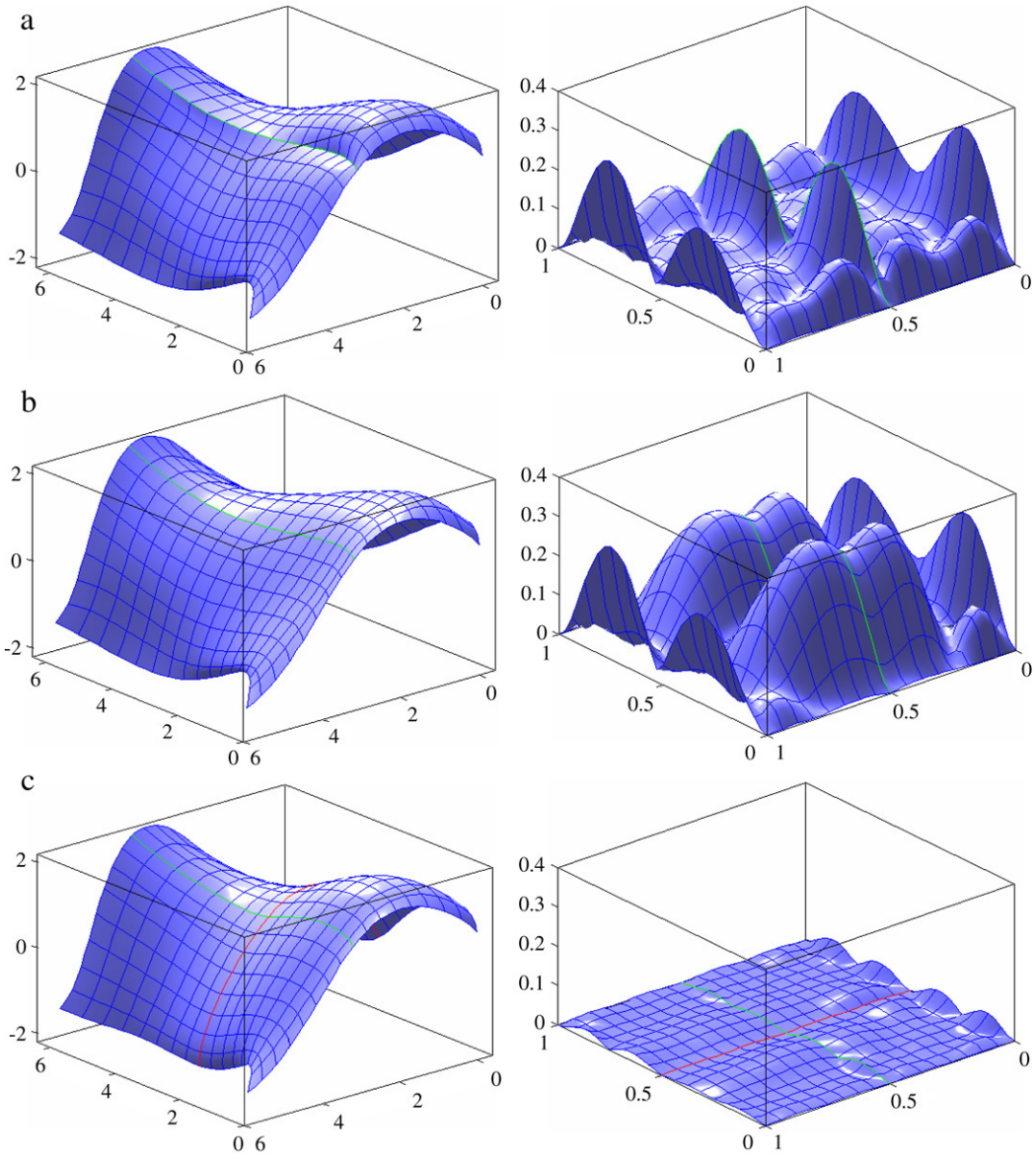

Fig. 5. Degree reduction of the surface patch in Fig. 4 from degree (6, 6) to degree (4, 4). In (b) and (c), the two patches are G^1 continuous.

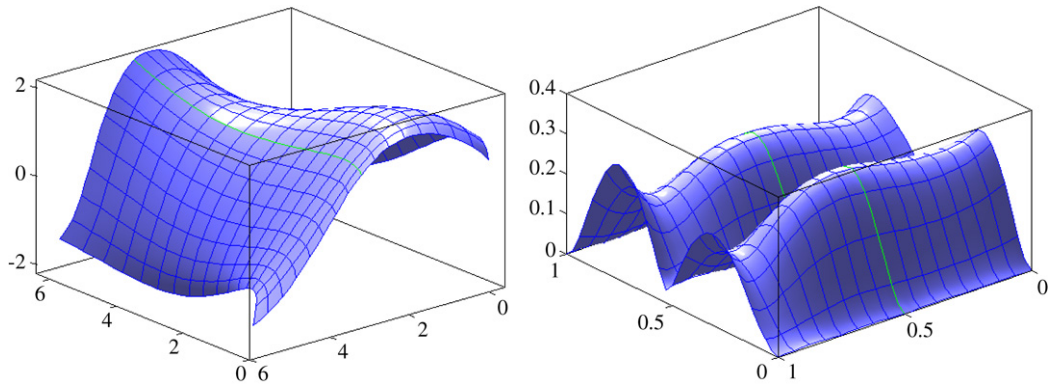

Fig. 6. Degree reduction of the surface patch in Fig. 4 from degree (6, 6) to degree (4, 4) by using the method in [7].

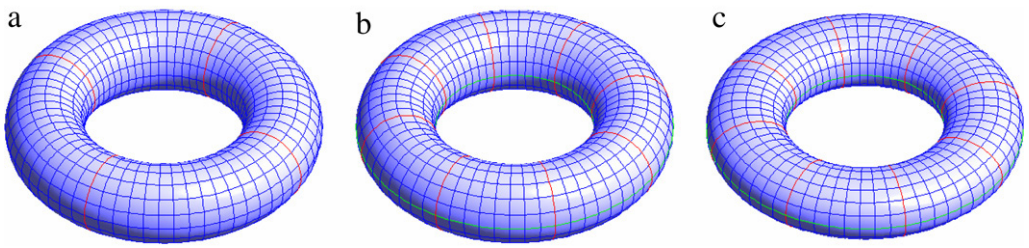

Fig. 7. The torus model. (a) 4 patches with degree (8, 8); (b) 16 patches with degree (4, 4); (c) 16 patches with degree (3, 3). The patches in (a) are C^1 continuous, while the patches in (b) and (c) are G^1 continuous and are obtained from (a) through subdivision and degree reduction.

Table 1
The mean and maximum errors of three examples.

	Fig. 5(a)	Fig. 5(b)	Fig. 5(c)	Fig. 6	Fig. 7(b)	Fig. 7(c)	Fig. 8(b)	Fig. 8(c)
$\varepsilon_{\text{mean}}$	5.775e−02	1.275e−01	7.709e−03	1.479e−01	1.184e−02	1.113e−01	6.746e−03	4.468e−03
$\varepsilon_{\max}$	2.991e−01	3.450e−01	3.895e−02	3.013e−01	2.044e−02	2.124e−01	1.919e−02	1.453e−02

In Fig. 6, we use the method in [7] to the two patches obtained by subdividing the patch in Example 1 at (0.5, 0). The approximations are achieved by applying the C^1-constrained degree reduction to every row and afterwards to every column of control nets. The maximum L_2-error of the two pairs of patches is 0.177. By comparing it with Fig. 5(b), and by the results in Table 1, we can see that the G^1-constrained approximation in this paper is better than the C^1-constrained one. This is because the G^1 constraint is much more relaxed in approximation problems.

Example 2. Consider the torus model parameterized as

$$\mathbf{T}(u, v) = \big((3 + \cos v)\cos u, (3 + \cos v)\sin u, \sin v\big), \quad u, v \in [0, 2\pi).$$

In Fig. 7(a), we approximate the torus by four C^1 tensor product Bézier patches of degree (8, 8) with high precision. Then, we obtain 16 patches of degree (8, 8) by subdividing every patch into four patches at the domain point (0.5, 0.5). Finally, we reduce the degree of the 16 patches to (4, 4) and (3, 3) in Figs. 7(b) and 7(c), respectively. And the approximating patches are adjusted by the scheme in Section 4.2.

Example 3. Consider the cup model, which is a surface of revolution and parameterized as

$$\mathbf{R}(u, v) = \big(\phi(v)\cos u, \phi(v)\sin u, \psi(v)\big), \quad u \in [0, 2\pi), \ v \in [0, 2],$$

where $(\phi(v), \psi(v))$ is represented by two C^1 Bézier curves of degree six, with the control points given by {(0.96, 0), (−0.16, 0.3), (0.47, 0.6), (0.08, 0.9), (0.19, 1.2), (0.39, 1.45), (0.61, 1.8)} and {(0.61, 1.8), (0.83, 2.15), (0.9, 2.24), (1.08, 2.8), (0.9, 2.85), (1.03, 3.25), (0.85, 3.5)}. In Fig. 8(a), we approximate the cup by two C^1 tensor product Bézier patches of degree (8, 8) with high precision. Then, we obtain 8 patches of degree (8, 8) by subdividing every patch into four patches at the domain point (0.5, 0.5). Finally, we reduce the degree of the 8 patches to (4, 4) in Fig. 8(b). In Fig. 8(c), the subdivision of each original patch is applied twice, so there are 32 patches, with the degree (3, 3). Similarly, the approximating patches obtained by degree reduction are adjusted by the scheme in Section 4.2.

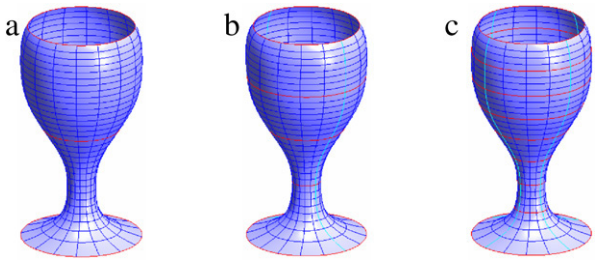

Fig. 8. The cup model. (a) 2 patches with degree (8, 8); (b) 8 patches with degree (4, 4); (c) 32 patches with degree (3, 3). The patches in (a) are C^1 continuous, while the patches in (b) and (c) are G^1 continuous and are obtained from (a) through subdivision and degree reduction.

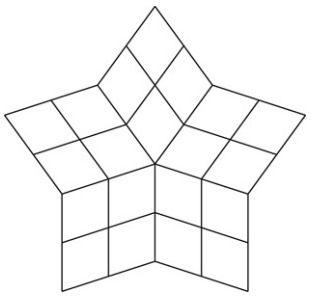

Fig. 9. An irregular domain whose center has valence 5.

Table 1 summarizes the numerical results of three examples. The mean errors $\varepsilon_{\text{mean}}$ and maximum errors $\varepsilon_{\max}$ are sampling-based estimates of various errors between the original patches and their approximating ones. More precisely, for every pair of patches, we take samples as follows:

$$\varepsilon_{i,j} = \left\| \mathbf{P}\left(\frac{i}{100}, \frac{j}{100}\right) - \mathbf{Q}\left(\frac{i}{100}, \frac{j}{100}\right) \right\|, \quad i, j = 0, 1, \ldots, 100.$$

6. Conclusion and future work

In this paper, we have considered constrained approximation of tensor product Bézier surfaces with special emphasis on the boundaries. By the position adjustment of some related control points after degree reduction, the resulting patches are smoothly joined with tangent plane continuity. So, we can trade off a little accuracy to achieve G^1-continuity.

Although the adjustment is simple and able to deal with surface patches defined on chessboard-like domains, it is a global scheme since the G^1 conditions are related to all the patches located on both sides of the boundaries for every direction. In future work, we plan to develop a local scheme such that the G^1 conditions depend only on the two patches on both sides of a common boundary and all the other patches incident to the two corners of the boundary. Moreover, we will be able to deal with surface patches defined on irregular domains, such as Fig. 9.

Acknowledgments

The author thanks the anonymous referees for their valuable suggestions and comments. This work is supported by the Science Fund for Young Scholars of Zhejiang Gongshang University.

References

[1] G. Farin, Curves and Surfaces for CAGD, 5th ed., Morgan Kaufmann, San Francisco, 2001.
[2] Y.J. Ahn, Using Jacobi polynomials for degree reduction of Bézier curves with C^k-constraints, Comput. Aided Geom. Design 20 (2003) 423–434.
[3] Y.J. Ahn, B.G. Lee, Y. Park, J. Yoo, Constrained polynomial degree reduction in the L_2-norm equals best weighted Euclidean approximation of Bézier coefficients, Comput. Aided Geom. Design 21 (2004) 181–191.
[4] G. Brunnett, T. Schreiber, J. Braun, The geometry of optimal degree reduction of Bézier curves, Comput. Aided Geom. Design 13 (1996) 773–788.
[5] J. Deng, Y. Feng, F. Chen, Best one-sided approximation of polynomials under L_1 norm, J. Comput. Appl. Math. 144 (2002) 161–174.
[6] M. Eck, Degree reduction of Bézier curves, Comput. Aided Geom. Design 10 (1993) 237–251.
[7] M. Eck, Least squares degree reduction of Bézier curves, Comput. Aided Design 27 (1995) 845–851.
[8] H.J. Kim, Y.J. Ahn, Good degree reduction of Bézier curves using Jacobi polynomials, Comput. Math. Appl. 40 (2000) 1205–1215.
[9] H.O. Kim, S.Y. Moon, Degree reduction of Bézier curves by L^1-approximation with endpoint interpolation, Comput. Math. Appl. 33 (5) (1997) 67–77.
[10] B.G. Lee, Y. Park, J. Yoo, Application of Legendre–Bernstein basis transformations to degree elevation and degree reduction, Comput. Aided Geom. Design 19 (2002) 709–718.

[11] L. Lu, G. Wang, Optimal multi-degree reduction of Bézier curves with G^2-continuity, Comput. Aided Geom. Design 23 (2006) 673–683.
[12] L. Lu, G. Wang, Application of Chebyshev II–Bernstein basis transformations to degree reduction of Bézier curves, J. Comput. Appl. Math. 221 (2008) 52–65.
[13] A. Rababah, B.G. Lee, J. Yoo, A simple matrix form for degree reduction of Bézier curves using Chebyshev–Bernstein basis transformations, Appl. Math. Comput. 181 (2006) 310–318.
[14] H. Sunwoo, Matrix representation for multi-degree reduction of Bézier curves, Comput. Aided Geom. Design 22 (2005) 261–273.
[15] B. Szafnicki, A unified approach for degree reduction of polynomials in the Bernstein basis Part I: Real polynomials, J. Comput. Appl. Math. 142 (2002) 287–312.
[16] M.A. Watkins, A.J. Worsey, Degree reduction of Bézier curves, Comput. Aided Design 20 (1988) 398–405.
[17] J. Zheng, G. Wang, Perturbing Bézier coefficients for best constrained degree reduction in the L_2-norm, Graphical Models 65 (2003) 351–368.
[18] G. Chen, G. Wang, Multi-degree reduction of tensor product Bézier surfaces with conditions of corners interpolations, Sci. China Ser. F 45 (2002) 51–58.
[19] M.A. Lachance, Chebyshev economization for parametric surfaces, Comput. Aided Geom. Design 5 (1988) 195–208.
[20] Q. Hu, G. Wang, Optimal multi-degree reduction of triangular Bézier surfaces with corners continuity in the norm L_2, J. Comput. Appl. Math. 215 (2008) 114–126.
[21] L. Lu, G. Wang, Multi-degree reduction of triangular Bézier surfaces with boundary constraints, Comput. Aided Design 38 (2006) 1215–1223.
[22] A. Rababah, Distance for degree raising and reduction of triangular Bézier surfaces, J. Comput. Appl. Math. 158 (2003) 233–241.
[23] J. Peters, U. Reif, Least squares approximation of Bézier coefficients provides best degree reduction in the L_2-norm, J. Approx. Theory 104 (2000) 90–97.
[24] P.J. Davis, Interpolation and Approximation, Dover Publications, New York, 1975.
[25] T.D. DeRose, Necessary and sufficient conditions for tangent plane continuity of Bézier surfaces, Comput. Aided Geom. Design 7 (1990) 165–179.
[26] P. Kiciak, Conditions for geometric continuity between polynomial and rational surface patches, Comput. Aided Geom. Design 13 (1996) 709–741.
[27] D. Liu, J. Hoschek, GC^1 continuity conditions between adjacent rectangular and triangular Bézier surface patches, Comput. Aided Design 21 (1989) 194–200.